Proton Nuclear Magnetic Resonance Assignments and Secondary Structure Determination of the ColE1 rop (rom) Protein

Wolfgang Eberle,[‡,⊥] Werner Klaus,[§] Giovanni Cesareni,[‡,‖] Chris Sander,[⊥] and Paul Rösch[*,‡,#]

Department of Biophysics, Max-Planck-Institute for Medical Research, Jahnstrasse 29, D-6900 Heidelberg 1, FRG, Gesellschaft für Biotechnologische Forschung, Mascherodeweg 1, D-3300 Braunschweig, FRG, and European Molecular Biology Laboratory (EMBL), Meyerhofstrasse 1, D-6900 Heidelberg 1, FRG

Received January 25, 1990; Revised Manuscript Received April 24, 1990

ABSTRACT: The complete resonance assignment of the ColE1 rop (rom) protein at pH 2.3 was obtained by two-dimensional (2D) proton nuclear magnetic resonance spectroscopy (^{1}H NMR) at 500 and 600 MHz using through-bond and through-space connectivities. Sequential assignments and elements of regular secondary structure were deduced by analysis of nuclear Overhauser enhancement spectroscopy (NOESY) experiments and $^3J_{HN\alpha}$ coupling constants. One 7.2-kDa monomer of the homodimer consists of two antiparallel helices connected by a hairpin loop at residue 31. The C-terminal peptide consisting of amino acids 59–63 shows no stable conformation. The dimer forms a four-helix bundle with opposite polarization of neighboring elements in agreement with the X-ray structure.

The ColE1 repressor of primer (rop,[1] 63 amino acids) protein acts in the control of plasmid replication by regulation of RNA–RNA interactions (Cesareni et al., 1985; Helmer-Citterich et al., 1988; Castagnoli et al., 1989). Processing of the precursor of the primer, RNAII, is inhibited by hydrogen bonding of RNAII to its complementary sequence in RNAI. rop increases the affinity of RNAI for RNAII and thus decreases the rate of replication initiation events. Because of this behavior, Tomizawa and Som (1984) named the protein rom (RNA one modulator).

The molecule exists as a dimer in the crystalline state as well as in aqueous solution as indicated by X-ray crystallography (Banner et al., 1987) and by its migration properties in a gel filtration column (Tomizawa & Som, 1984). The tertiary structure of the protein is intact even at elevated temperature, the melting temperature being 316 K, at intermediate pH, and is stable at acidic pH down to pH 2.0 as shown by microcalorimetry (H.-J. Hinz, personal communication). This temperature and acid stability makes it particularly suitable for structural studies employing two-dimensional (2D) proton nuclear magnetic resonance (^{1}H NMR) spectroscopy. Genetic engineering methods are being used to obtain mutant proteins in high amounts and high purity for NMR investigations. These include attempts to engineer a copper binding site (up to six point mutations) and to provide a unique antigenic recognition site (Emery et al., 1990). X-ray crystallography has yielded the structure of mutants with a deletion of five and an insertion of two residues in the loop region and a decrease of the size of side chains (L > V > A) in the protein core at residues 41 and 48 (Kokkinidis et al., 1987; Castagnoli et al., 1989).

Over the last few years, NMR clearly has become an alternative tool for the determination of 3D protein structures in solution (Wüthrich, 1986) for molecules up to about 100 amino acids. We have performed, as a first step toward the determination of the three-dimensional structure of the rop protein in solution, resonance assignments in the ^{1}H NMR spectrum of the rop protein. In addition, we were able to assign secondary structure elements.

MATERIALS AND METHODS

Sample Preparation and Experimental Conditions. The protein was prepared as described by Banner et al. (1983). A series of one-dimensional measurements under various temperature and pH conditions led to the definition of the optimal experimental conditions, 308 K and pH 2.3. After the standard preparation (Banner et al., 1987), which resulted in a protein solution close to pH 7, protein was lyophilized, redissolved in 5 mL of 1 M phosphoric acid, pH 2.3, and extensively dialyzed against 5 mM phosphoric acid, pH 2.3. Subsequently, the protein was lyophilized and redissolved either in D$_2$O ("100%" D$_2$O from Sigma) or in 10% D$_2$O/90% H$_2$O to the desired concentration. Measurements were performed on approximately 10 mM protein solutions in D$_2$O and in a mixture consisting of D$_2$O and H$_2$O with about 50 mM sodium phosphate buffer. Dimethylsilylsulfonic acid (DSS) was used as internal reference.

NMR. Two series of 2D experiments were performed both in H$_2$O and in D$_2$O on a commercial Bruker AM 500 spectrometer working at a proton resonance frequency of 500 MHz: double quantum filtered correlated spectroscopy (DQF-COSY; Rance et al., 1983), nuclear Overhauser enhancement spectroscopy (NOESY; Bodenhausen et al., 1984), and total correlated spectroscopy (TOCSY; Braunschweiler & Ernst, 1983; Davies & Bax, 1985) with WALTZ-16 mixing cycles (Rance, 1987) were performed with mixing times of 150, 200, and 300 ms for the NOESY and 40, 60, and 90 ms for the TOCSY experiments. These spectra were acquired in the phase-sensitive mode with quadrature detection in both di-

---

[‡] Max-Planck-Institute for Medical Research.
[⊥] European Molecular Biology Laboratory.
[§] Gesellschaft für Biotechnologische Forschung.
[‖] Present address: Dipartmento di Biologia, II Universita di Roma, Torvergata, Via Orazio Raimondo, Roma, Italy.
[#] Permanent address: Department of Structure and Chemistry of Biopolymers, P.O. Box 101251, D-8580 Bayreuth, FRG.

[1] Abbreviations: COSY, correlated spectroscopy; 1D, 2D, one dimensional, two dimensional; DQF-COSY, double quantum filtered COSY; DSS, 2,2-dimethyl-2-silapentanesulfonate; FID, free induction decay; NMR, nuclear magnetic resonance; NOE, nuclear Overhauser effect; NOESY, nuclear Overhauser enhancement spectroscopy; RELAYED-COSY, relayed coherence transfer spectroscopy; rom, RNA one modulator; rop, repressor of primer; TOCSY, total coherence transfer spectroscopy; TPPI, time proportional phase incrementation.

mensions using the time proportional phase incrementation technique (TPPI; Marion & Wüthrich, 1983). RELAYED-COSY experiments (Wagner, 1983) with mixing times of 20 and 40 ms were performed in the magnitude mode.

Three spectra in H_2O were recorded at a proton resonance frequency of 600 MHz with a Bruker AM 600 spectrometer at the Gesellschaft für Biotechnologische Forschung, Braunschweig: DQF-COSY, NOESY with 75-ms mixing time, and CLEAN-TOCSY (Griesinger et al., 1988), since the cross-relaxation peak suppression with this technique proved to be superior to the standard TOCSY experiment. CLEAN-TOCSY spectra were acquired without trim pulses with 60-ms mixing time. Solvent resonance suppression was performed by permanent coherent irradiation prior to the first excitation pulse and during the mixing time in the NOESY experiment.

For the qualitative determination of the amide proton exchange rate, a 2D NOESY experiment was performed: mixing time, 75 ms; $T = 300$ K; pH 2.3; total duration of the experiment, 17 h. The protein was freshly prepared in H_2O, lyophilized, and then dissolved in D_2O.

Acquisition and Processing Parameters. The spectral width was around 6 kHz in all experiments. A total of 512 t_1 increments with 2-kb complex data points were recorded per experiment.

A $\pi/8$ shifted sine-bell filter was applied in the t_1 and t_2 dimension before Fourier transformation. For all TOCSY experiments, application of a cosine squared filter together with spline base-line correction after Fourier transformation in both dimensions yielded the best results in terms of the number of detectable cross-peaks.

In the t_2 dimension only 1-kb complex data points were used and zero-filled to yield 2-kb data points after Fourier transformation. This resulted in the best combination of resolution and signal to noise ratio (Bartholdie & Ernst, 1973). In the t_1 dimension, the data matrix was zero-filled to 1 kb.

$^3J_{NH\alpha}$ coupling constants were extracted from a 1D NMR spectrum recorded at 600 MHz with 16-kb complex data points. The free induction decay (FID) was resolution-enhanced by multiplication with a Gaussian function and zero-filled before Fourier transformation to yield 32-kb data points. Processing was performed on a commercial Bruker Aspect 3000 or on a Convex 210 computer networked with Silicon Graphics IRIS workstations using home-written software in the C programming language based in part on a package supplied by Prof. R. Kaptein, Utrecht, and Dr. R. Scheek, Groningen. Some display and plotting routines of the software package "AURELIA" running on a Bruker X-32 computer were used.

RESULTS AND DISCUSSION

Assignment Strategy. Sequence-specific assignment of resonances was performed in six steps. The procedure involves major aspects of the main-chain-directed approach (Englander & Wand, 1987) and is based on the idea that the information gained from a knowledge of the assignment of the backbone amide proton, $C_\alpha H$, and $C_\beta H$ resonances is sufficient to define regular secondary structure elements (Wüthrich et al., 1984).

Step 1: Assignment of the Backbone Amide Proton, $C_\alpha H$, and $C_\beta H$ Resonances. By brief inspection of the COSY, RELAYED-COSY, and TOCSY spectra in H_2O (Figure 1), the NH, $C_\alpha H$, and $C_\beta H$ resonances were identified except for the spin systems of 48L, 49Y, and 52C.

Step 2: Recognition of Patterns of Regular Secondary Structure. Strong NH–NH cross-peaks indicated a nearly complete helical structure in the H_2O NOESY spectrum of the rop protein. It was possible to define chains of up to 12
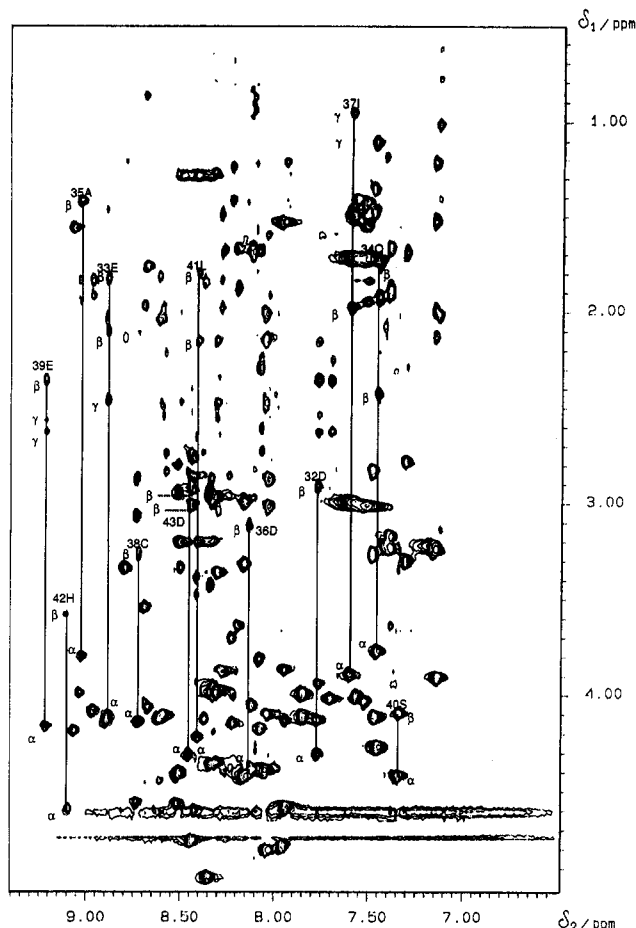

FIGURE 1: Part of a 600-MHz CLEAN-TOCSY spectrum; mixing time, 60 ms; [protein], 10 mM; phosphate buffer, 50 mM; pH 2.3; $T = 308$ K. The spin system assignment from 32D to 43D is indicated.
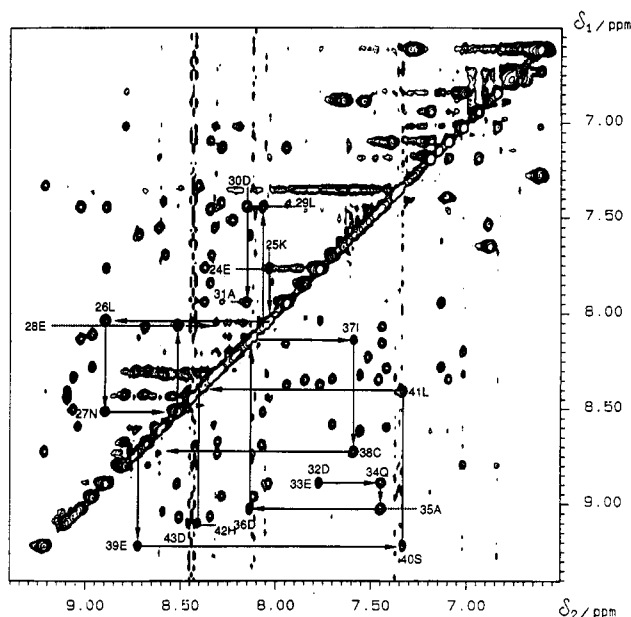

FIGURE 2: 600-MHz NOESY spectrum in H_2O, mixing time 75 ms. The NH–NH connectivities from 32D to 43D and from 24E to 31A are outlined. These connectivities are indicative of helical structures and are a good starting point for further secondary structure element analysis. Experimental conditions as in Figure 1.

sequential residues linked by strong NH–NH nuclear Overhauser effects (NOEs) (Figure 2). The chains terminate at frequency degeneracies of the backbone amide protons with one exception, 31A–32D. In this protein region, two strong sequential $C_\alpha H$–NH NOEs occur: 31A–32D and 32D–33E.
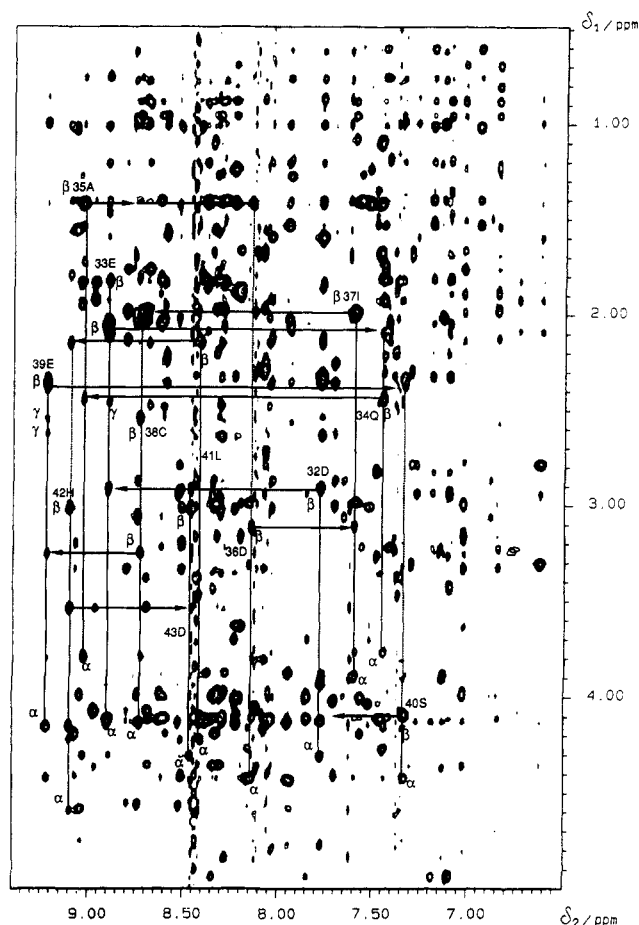
FIGURE 3: Part of the spectrum in Figure 2. The intraresidue NOEs NH–C_αH, NH–C_βH, and NH–C_γH are indicated by vertical lines. Horizontal lines show sequential C_βH–NH connectivities from 32D to 43D.

A third strong NOE can be detected between 2T and 3K, immediately at the start of the first helix. All other sequential NOEs of this type were markedly weaker.

Further indications of helical structures in the rop protein spectra were strong intraresidue NH–C_βH cross-peaks, sequential C_βH–NH cross-peaks (Figure 3), weak or medium sequential C_αH–NH cross-peaks, medium-range C_αH(i)–NH(i+3) cross-peaks, medium-range NH(i)–NH(i+2) cross-peaks, medium-range C_αH(i)–C_βH(i+3) cross-peaks, and $^3J_{NHC\alpha}$ coupling constants smaller than 6 Hz. The $^3J_{NHC\alpha}$ coupling constants were interpreted in terms of Φ torsion angle restraints of $-90° < \Phi < -40°$ (Pardi et al., 1984). C_αH(i)–HN(i+4) cross-peaks were found along nearly the whole length of the helical parts, clearly indicating α-helical structures. Only the C_αH(28)–NH(30) cross-peak at the C-terminal end of the first helix suggests 3_{10} character of the helix. The results are summarized in Figure 4. The nearly complete chain of sequential C_βH–NH NOEs corroborates the sequential connectivities derived from the sequential NH–NH NOEs.

Step 3: Recognition of the Spin Systems Using Through-Bond Connectivities (Wüthrich, 1986). This step was performed by parallel analysis of DQF-COSY, RELAYED-COSY, and TOCSY experiments, independent from the search for secondary structure elements. The easiest starting point was the TOCSY spectra recorded in H_2O. The cross-peaks due to connectivities between backbone amide protons and C_αH, C_βH, C_γH, or C_δH delivered sets of resonances belonging to the same residue. With the aid of DQF-COSY and RELAYED-COSY experiments, it was possible to arrange these single sets according to the 10 different spin system patterns

in about 75% of all cases in the first attempt.

All six alanine spin systems could be identified on the basis of their very strong NH–C_βH RELAY cross-peaks and the characteristic fine structure of the C_αH–C_βH COSY cross-peaks. Resonances of two out of the four threonines (7T, 21T) could be identified on the basis of their C_αH–C_γH RELAY cross-peaks at the typical frequency values (Gross & Kalbitzer, 1988; Wüthrich, 1986). The 57G resonance assignments could be achieved via the two NH–C_αH DQF-COSY cross-peaks. In the TOCSY spectrum, these two peaks showed significantly higher intensity. The key for the elucidation of the extended networks of arginine and lysine spin systems were the H_2O–COSY cross-peaks linking side chain amide proton resonances to C_δH and C_ϵH resonances, respectively. TOCSY cross-peaks between backbone and side chain amide protons and C_βH, C_γH, and C_δH groups completed the assignment of resonances of the 13R, 16R, and 50R spin systems as well as the 3K and 6K spin systems. The assignments of the resonances of the 55R and 25K spin systems were postponed because of the difficulties introduced by the frequency degeneration of their side chain amide protons. Three AMX systems with aromatic side chains (42H, 44H, 56F) could be identified due to NOEs from C_δH to C_βH according to Billeter et al. (1982). However, no connections between an AMX spin system and the aromatic ring spin system of 14F could be identified, because all aromatic ring proton resonances and the C_δH proton resonances from the imidazole ring of 44H were frequency-degenerated. The assignment of the 49Y resonances was postponed because both the NH–C_αH and NH–C_βH cross-peaks overlap with other signals. The protons of 10N and 27N show well-resolved complete AMX patterns and could be separated from the other AMX systems on the basis of their NOEs between side chain amide protons and C_βH. 17S and 40S, 38C and 30D, 32D, 36D, and 58D could be identified from TOCSY cross-peaks at typical ppm values. 51S, 43D and 46D, and 52C were identified at a later stage. Identification of the AM(PT)X systems in this step was possible in eight cases: 24E, 28E, 33E, 39E, 47E, 11M, and 34Q. 4Q, 18Q, and 5E were assigned later. The spin systems of two isoleucines and all but two leucines, 26L and 48L, were identified.

Step 4: Combination of the Information from Previous Steps and the Knowledge of the Amino Acid Sequence in Order To Place the Helical Segments into the Sequence. Comparison of the chains of sequential spin systems with the amino acid sequence led to unique sequence-specific assignments except in the region 49Y–53L. No NH–NH NOEs could be detected in this region because of frequency degeneration of the resonances. Thus, these assignments were made at the end of the whole procedure. The chemical shifts of the assigned resonances are summarized in Table I.

Step 5: Completion of the Spin System Assignments. Analysis of the very crowded regions in the aliphatic part of the spectra of the rop protein then led to safe assignments of all proton resonances from residue 2T to residue 58D. Two different local conformations around cysteine-52 are possible, as is evident from the observation of two frequency values for the C_αH of this residue. Both signals are highfield-shifted and coupled through exchange peaks. The intensity of NOEs from C_αH of both conformations to neighboring protons is slightly different in each case. The NOE connectivities in Figure 4 are due to the C_αH signal at lower field.

No resonances could be assigned for the N-terminal methionine and the C-terminal sequence 59G–63L. Obviously, the C-terminal piece of the protein has no strictly defined conformation in solution, not different from the crystal

Table I: ^{1}H Chemical Shifts and Assignments of rop (rom) at pH 2.3, 308 K[a]

residue	NH	C$_\alpha$H	C$_\beta$H	C$_\gamma$H	C$_\delta$H	others
M 1						
T 2	7.94	4.58	4.76	1.27		
K 3	9.04	3.99	1.95, 1.83	1.55, 1.44	1.73	C$_\epsilon$H, 3.01 N$_\zeta$H, 7.51
Q 4	8.60	4.12	2.03, 1.95	2.54, 2.48		N$_\epsilon$H, 6.83
E 5	7.42	3.21	2.06	1.18		
K 6	8.29	3.97	1.50	1.51	1.83	C$_\epsilon$H, 2.98 N$_\zeta$H, 7.59
T 7	8.32	3.99	4.19	1.27		
A 8	7.56	4.00	1.41			
L 9	8.62	4.12	2.05, 1.81	1.89	0.95, 0.88	
N 10	8.74	4.62	3.06, 2.88			N$_\delta$, 7.66 6.88
M 11	8.30	4.36	2.47, 2.15	2.55		
A 12	8.68	4.06	1.76			
R 13	8.80	3.33	2.12, 1.98	1.53, 1.21	3.23	N$_\epsilon$H, 7.15 aromatic 7.37
F 14	8.42	4.60	3.47, 3.38			
I 15	8.69	3.54	1.97	C$_\gamma$H$_3$, 0.87 C$_\gamma$H$_2$, 1.02 0.99	0.78	
R 16	8.07	3.81	2.20, 1.67	1.67	3.31, 2.79	N$_\epsilon$H, 7.30
S 17	8.11	4.37	4.06			
Q 18	8.97	4.07	1.92, 1.83			N$_\epsilon$H, 7.37
T 19	8.28	3.88	4.84	1.41		
L 20	7.13	3.90	2.01, 1.00	1.41	0.78, 0.63	
T 21	7.95	3.87	4.13	1.21		
L 22	8.37	4.12	1.85	1.41	1.01, 0.89	
L 23	7.77	3.94	2.33, 2.13	1.60	1.00, 0.87	
E 24	7.70	4.12	2.63, 2.54			
K 25	8.03	4.11	1.91	1.35, 1.11	1.60	C$_\epsilon$H, 2.93 2.83 N$_\zeta$H, 7.48
L 26	8.91	4.13	2.04	2.04	1.02, 0.75	
N 27	8.52	4.57	2.93, 2.79			N$_\delta$H, 7.28 6.62
E 28	8.07	4.17	2.29, 2.22	2.72, 2.60		
L 29	7.44	4.27	1.92	1.82	0.76, 0.60	
D 30	8.15	4.43	3.31, 2.99			
A 31	7.95	4.77	1.53			
D 32	7.77	4.30	3.03, 2.91			
E 33	8.89	4.10	2.10, 1.82	2.46		
Q 34	7.45	3.77	2.44, 1.74	2.31, 2.22		N$_\epsilon$H, 7.10 7.38
A 35	9.03	3.79	1.42			
D 36	8.14	4.42	3.11			
I 37	7.59	3.89	1.99	C$_\gamma$H$_3$, 0.95 C$_\gamma$H$_2$, 2.93	0.88	
C 38	8.73	4.14	3.25, 2.54			
E 39	9.22	4.15	2.36	2.62, 2.55		
S 40	7.34	4.42	4.09			
L 41	8.41	4.22	2.15, 1.80	1.73	1.03, 1.01	
H 42	9.10	4.61	3.54, 3.02			C$_\delta$H, 8.46 C$_\epsilon$H, 8.75
D 43	8.45	4.31	3.02, 2.91			
H 44	8.51	4.41	3.33, 3.20			C$_\delta$H, 7.35 C$_\epsilon$H, 8.62
A 45	9.06	4.19	2.88			
D 46	8.34	4.36	2.88			
E 47	7.70	4.02	2.36, 2.25	2.62		
L 48	8.61	4.44	2.22	1.57	0.88, 0.75	
Y 49	8.32	3.97	3.16, 3.00			C$_\delta$H, 7.02 C$_\epsilon$H, 6.84
R 50	8.20	3.63	1.88	1.89, 1.66	3.23, 3.17	N$_\epsilon$H, 7.39
S 51	8.22	4.15	4.09, 4.01			
C 52	8.30	3.36, 3.00[b]	2.65, 2.33			
L 53	8.23	3.70	1.42, 1.24	1.24	0.80, 0.70	
A 54	7.52	4.03	1.42			
R 55	7.46	4.11	1.68, 1.10	1.76, 1.35	3.27, 2.83	N$_\epsilon$H, 7.48 C$_\delta$H, 7.10 C$_\epsilon$H, 7.19 C$_\zeta$H, 6.94
F 56	8.35	4.94	3.43, 2.94			
G 57	7.85	4.11, 4.00				
D 58	8.03	4.80	3.01, 2.87			
D 59						
G 60						
E 61						
N 62						
L 63						

[a] Chemical shifts in ppm from internal DSS; accuracy ±0.01 ppm. [b] Two conformations for 52C were observed leading to two values for the C$_\alpha$ proton.
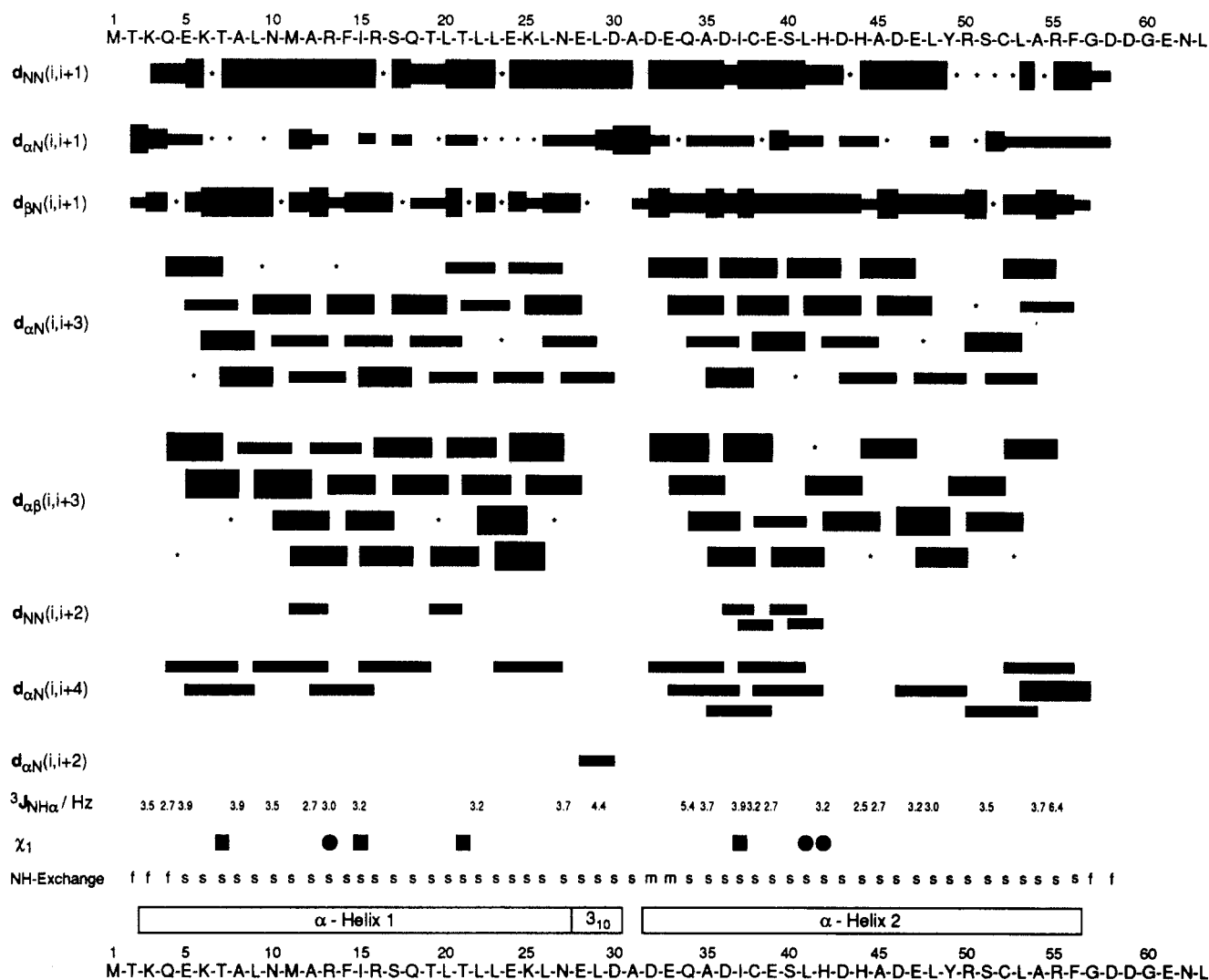
M-T-K-Q-E-K-T-A-L-N-M-A-R-F-I-R-S-Q-T-L-T-L-L-E-K-L-N-E-L-D-A-D-E-Q-A-D-I-C-E-S-L-H-D-H-A-D-E-L-Y-R-S-C-L-A-R-F-G-D-D-G-E-N-L

$d_{NN}(i,i+1)$

$d_{\alpha N}(i,i+1)$

$d_{\beta N}(i,i+1)$

$d_{\alpha N}(i,i+3)$

$d_{\alpha \beta}(i,i+3)$

$d_{NN}(i,i+2)$

$d_{\alpha N}(i,i+4)$

$d_{\alpha N}(i,i+2)$

$^3J_{NH\alpha}$ / Hz   3.5 2.7 3.9   3.9   3.5   2.7 3.0   3.2   3.2   3.7   4.4   5.4 3.7   3.9 3.2 2.7   3.2   2.5 2.7   3.2 3.0   3.5   3.7 6.4

χ_1

NH-Exchange   f f f s s s s s s s s s s s s s s s s s s s s s s s s s s s s m m s s s s s s s s s s s s s s s s s s s s s s s s s s s f f

α - Helix 1   3₁₀   α - Helix 2

M-T-K-Q-E-K-T-A-L-N-M-A-R-F-I-R-S-Q-T-L-T-L-L-E-K-L-N-E-L-D-A-D-E-Q-A-D-I-C-E-S-L-H-D-H-A-D-E-L-Y-R-S-C-L-A-R-F-G-D-D-G-E-N-L

FIGURE 4: Sequence of ColE1 rop with a survey of interresidue NOEs which are relevant for secondary structure determination, $^3J_{NH\alpha}$ coupling constants (accuracy ±0.4 Hz), χ_1 side chain torsion angles, and NH exchange rates. The derived secondary structure is shown at the bottom. The thickness of the lines corresponds to the magnitudes of the NOEs, i.e., weak, medium, and strong. An asterisk indicates that the NOE could not be observed because of frequency degeneracy. The χ_1 side chain torsion angles were derived from $^3J_{\alpha\beta}$ coupling constants and intraresidue NOE intensity patterns: (●) $120° < \chi_1 < 240°$; (■) $240° < \chi_1 < 360°$. The amide proton exchange rates were qualified according to a 2D-NOESY experiment as described in the main text. "s" indicates low and "f" indicates high exchange rates. "m" denotes medium values.

structure (Banner et al., 1987).

Step 6: Analysis of Nonsequential Cross-Peaks in the NOESY Spectra. The assignment of interresidue short- and medium-range NOEs confirms the previous assignments. A few cross-peaks, e.g., between residues 8 and 56 or residues 20 and 42, indicate an antiparallel alignment of the two helices. Under this assumption, all remaining NOEs could be separated into long-range connectivities inside a monomer and those determining the global conformation of the dimer, the latter cross-peaks being rather scarce. As is shown in the contact map in Figure 5, the two classes of long-range NOEs set up a characteristic pattern of connectivities.

By this procedure, about 98% of the NOESY cross-peaks could be assigned consistently. The NOESY experiment in D_2O performed immediately after dissolving the protein in D_2O showed that most of the amide hydrogens have very low exchange rates, as postulated for hydrogens participating in buried hydrogen bonds: For residues 5E–31A and 34Q–56F, all NOEs from backbone NH to hydrogens in the same or other residues arise with about the same intensity as in the NOESY experiments in H_2O. Of the cross-peaks originating from the backbone amide protons of 32D and 33E, only the sequential NH–NH NOE between these residues could be observed with an intensity just at the limit of detectability.

NOEs for the amide protons from residues 2T, 3K, 4Q, 57G, and 58D could be detected no longer, indicating fast exchange of these protons.

The determination of some χ_1 side chain torsion angles was performed based on qualitative interpretation of intraresidue NOE intensities (NH–C_βH and C_αH–C_βH) and on values of the $^3J_{\alpha\beta}$ coupling constants (Wagner et al., 1987). The results are summarized in Figure 4.

Structure. As outlined in Figure 6, the monomer consists of two helical parts connected by a hairpin loop. The series of C_αH(i)–NH($i+3$) and C_αH(i)–C_βH($i+3$) NOEs define the helical segments as 4Q–30D and 32D–56F. Most probably, although not strictly by the criteria listed in step 2, the first helix starts at residue 3K. The NOE connectivities for C_αH(3)–NH(6), C_αH(3)–C_βH(6), and C_αH(3)–NH(7) are degenerate with other signals and therefore could not be identified. The amide protons of the first three residues of an α-helix are not involved in backbone hydrogen bonds and thus are expected to show high exchange rates. This is the case for 3K and 4Q, but not for 5E. Observed NOEs between 2T and 5E lead to the hypothesis that the side chain oxygen of 2T and the backbone NH of 5Q are hydrogen-bonded. This type of start of a helix was also found in the antennapedia homeodomain (Otting et al., 1988). The first helix is an
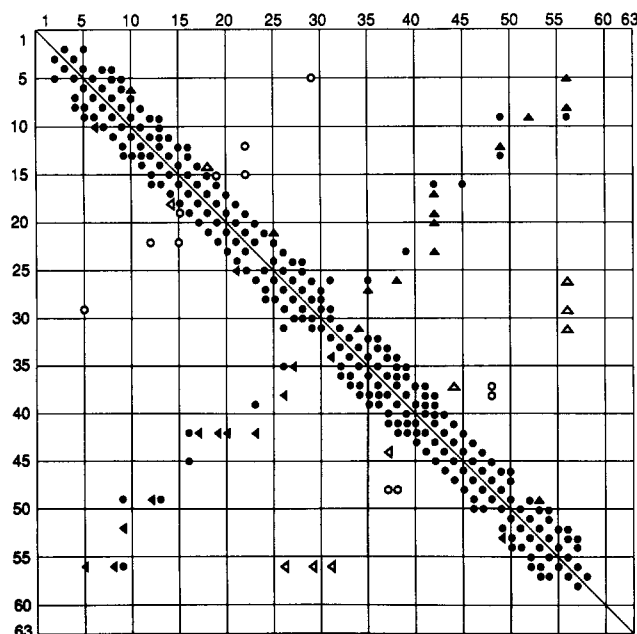
FIGURE 5: Contact map. Filled circles (●) indicate NOEs inside a monomer where at least one proton is a backbone proton. If both protons belong to side chains, the NOEs inside a monomer are shown as filled triangles (▲). For NOEs determining the global dimer configuration, open circles (O) and open triangles (△) have the same meaning as above.
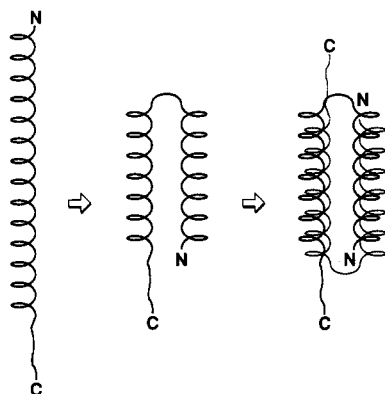

FIGURE 6: Schematic drawing of the structure of rop (rom). The monomer consists of two antiparallel helices, 3K–30D and 32D–56F which are connected with a sharp hairpin loop. The dimer contains two antiparallel monomers arranged as shown, forming thereby a four-bundle helix motif.

α-helix except in the last turn, where 3_{10} character is detected. The sharp hairpin loop could not be classified as a standard turn; the NOEs do not match any pattern expected from common loops (Wagner et al., 1986). The second helix is pure α type. 57G does not belong to the α-helix as judged from the amide proton's fast exchange rate.

The NOEs determining the packing of the α-helices 1 and 2 show a staircase pattern with step width seven, i.e., the period of a heptad sequence of a coiled-coiled four α-helix bundle.

About 50 long-range NOEs between the 2 helices over their whole length confirm their antiparallel arrangement. In total, about 400 intra- and 400 interresidue NOEs could be assigned; 20 NOEs indicate the motif of four-bundle helices of the dimer. Detailed discussions of the tertiary and quaternary structure have to await the results of distance geometry and molecular dynamics calculations currently under way.

REFERENCES

Banner, D. W., Cesareni, G., & Tsernoglou, D. (1983) *J. Mol. Biol. 170*, 1059–1060.

Banner, D. W., Kokkinidis, M., & Tsernoglou, D. (1987) *J. Mol. Biol. 196*, 657–675.

Bartholdie, E., & Ernst, R. R. (1973) *J. Magn. Reson. 11*, 9–19.

Bax, A., & Davies, D. G. (1985) *J. Magn. Reson. 65*, 355–366.

Billeter, M., Braun, W., & Wüthrich, K. (1982) *J. Mol. Biol. 155*, 321–346.

Bodenhausen, G., Kogler, H., & Ernst, R. R. (1984) *J. Magn. Reson. 58*, 370–388.

Braunschweiler, L. R., & Ernst, R. R. (1983) *J. Magn. Reson. 53*, 521–528.

Castagnoli, L., Scarpa, M., Kokkinidis, M., Banner, D. W., Tsernoglou, D., & Cesareni, G. (1989) *EMBO J. 8*, 621–629.

Cesareni, G., & Banner, D. W. (1985) *Trends Biochem. Sci. (Pers. Ed.) 10*, 303–306.

Emery, S. C., Blöcker, H., Cesareni, G., Kingswell, A., & Sander, C. (1990) *Protein Eng.* (in press).

Englander, S. W., & Wand, A. J. (1987) *Biochemistry 26*, 5953–5958.

Griesinger, C., Otting, G., Wüthrich, K., & Ernst, R. R. (1988) *J. Am. Chem. Soc. 110*, 7870–7872.

Gross, K. H., & Kalbitzer, H. R. (1988) *J. Magn. Reson. 76*, 87–99.

Helmer-Citterich, M., Anceschi, M. M., Banner, D. W., & Cesareni, G. (1988) *EMBO J. 7*, 557–566.

Kokkinidis, K., Cesareni, G., Helmer-Citterich, M., Castagnoli, L., Scarpa, M., Tsernoglou, D., & Banner, D. W. (1987) *Protein Eng. 1*, 244.

Marion, D., & Wüthrich, K. (1983) *Biochem. Biophys. Res. Commun. 113*, 967–974.

Otting, G., Qian, Y., Müller, M., Affolter, M., Gehring, W., & Wüthrich, K. (1988) *EMBO J. 7*, 4305–4309.

Pardi, A., Billeter, M., & Wüthrich, K. (1984) *J. Mol. Biol. 180*, 741–751.

Rance, M. (1987) *J. Magn. Reson. 74*, 557–564.

Rance, M., Sorensen, O. W., Bodenhausen, G., Wagner, G., Ernst, R. R., & Wüthrich, K. (1983) *Biochem. Biophys. Res. Commun. 117*, 479–485.

Tomizawa, J., & Som, T. (1984) *Cell 38*, 871–878.

Wagner, G. (1983) *J. Magn. Reson. 55*, 151–156.

Wagner, G., Neuhaus, D., Wörgötter, E., Vasak, M., & Wüthrich, K. (1986) *J. Mol. Biol. 187*, 131–135.

Wagner, G., Braun, W., Havel, T. F., Schaumann, T., Go, N., & Wüthrich, K. (1987) *J. Mol. Biol. 196*, 611–639.

Wüthrich, K. (1986) *NMR of Proteins and Nucleic Acids*, Wiley, New York.

Wüthrich, K., Billeter, M., & Braun, W. (1984) *J. Mol. Biol. 180*, 715–740.